Electropolymerized AIE-Active Polymer Film with High Quantum Efficiency and its Application in OLED

Jinyu Li,[1] Xiao Han,[1] Qing Bai,[1] Tong Shan,[1] Ping Lu,[1] Yuguang Ma[2]

[1]State Key Laboratory of Supramolecular Structure and Materials, Jilin University, 2699 Qianjin Avenue, Changchun 130012, China

[2]Institute of Polymer Optoelectronic Materials and Devices, State Key Laboratory of Luminescent Materials and Devices, South China University of Technology, Guangzhou 510640, China

Correspondence to: P. Lu (E-mail: lup@jlu.edu.cn)

Received 31 August 2016; accepted 18 October 2016; published online 00 Month 2016

DOI: 10.1002/pola.28414

ABSTRACT: A carbazole functionalized electro-active AIE-activity molecule, **TPE-DFCz**, was designed, synthesized, and well characterized. The clear difference in oxidation potentials between tetraphenylethylene (TPE) unit and carbazole groups was found which guaranteed that polymerization occurred only at the peripheral carbazole groups and the TPE unit remained unchanged. Its luminescent network film was prepared conveniently by electrochemical polymerization (EP). The cross-linked film exhibited green emission with high quantum efficiency of 63%, relatively smooth surface, and good thermal stability. The effect of different scan cycles on the optical property was also investigated. The electroluminescent device using the optimized polymer film as active layer showed a maximum luminance of 3200 cd m^{-2} and a maximum luminance efficiency of 1.16 cd A^{-1} with very low roll-off of the efficiency. The AIE-active EP films afford more opportunities to develop polymer films with high quantum efficiency via a simple, effective method and promote the potential applications in display devices. © 2016 Wiley Periodicals, Inc. J. Polym. Sci., Part A: Polym. Chem. **2016**, *00*, 000–000

KEYWORDS: aggregation-induced emission; efficiency; electrochemical polymerization; electrochemistry; luminescence; OLEDs; polymers; tetraphenylethylene

INTRODUCTION Great achievements have been made in organic light-emitting materials over the past decades due to their wide applications in optoelectronic fields such as organic light-emitting diodes (OLEDs),[1–4] organic field-effect transistors (OFETs),[5–8] and organic photovoltaic devices (OPVs).[9–11] Conjugated polymers are regarded as the most promising candidates because they can be prepared conveniently by low-cost technologies for the fabrication of optoelectronic devices.[12,13] Several methods including spin-coating,[14] ink-jet printing,[15] and electrochemical polymerization (EP)[16] are generally utilized to prepare polymer films. Creation of polymer films with long-term stability under device operating conditions is of significant importance. In this case, EP method is a promising approach to afford luminescent cross-linked network with ideal stability by fixing the positions and phase of polymer chains,[17] which has already shown great potentials in supercapacitors,[18] fluorescence detection of TNT,[19] and electrode modifying interlayer.[20–22] In addition, the *in situ* polymerization avoids the complicated synthesis process of polymer and reduces the waste of materials during film fabrication. Furthermore, polymer film can be deposited directly onto the conducting substrates with various sizes and geometries by electrochemically oxidizing suitable electro-active precursors.[23–25] The growth rate and thickness of the polymer films are also controllable by conveniently regulating applied potential and total amount of charge passed through the cell, respectively.[26–28] All these features endow EP as an ideal method to prepare cross-linked polymer films with good stability.

Another factor that needs to take into consideration is the high efficiency in solid state, which is very important to promote the application in OLEDs. Most traditional light-emitting materials suffer from the aggregation-caused quenching (ACQ) effect in high-concentration solution or in solid state due to the strong π-π interactions.[29] A particular phenomenon that materials show almost no emission in solution but emit strongly in condensed media, named as aggregation-induced emission (AIE), was firstly discovered by Luo et al. in 2001.[30] This new phenomenon provides a unique way to obtain organic conjugated materials with high quantum efficiency in aggregated state. Tetraphenylethylene (TPE) is a classical chromophore which possesses a simple structure but shows a splendid AIE property.[31,32] The facile

Additional Supporting Information may be found in the online version of this article.

synthesis and ready functionalization have made it a mostly investigated building block catering to the needs of a wide range of high technological applications.[33] Up to date, efficient fluorescent blue, green, red, and white OLEDs materials have been prepared using TPE as a versatile constructing unit.[34] Carbazole is a commonly utilized organic luminescent material with good hole-injection ability and high thermal stability.[35,36] Carbazole also behaves as a highly electro-active group with a relatively low oxidation potential.[37–39] Very effective coupling between its oxidative species of carbazyl radical cation, and structurally well-defined coupling products of dimeric carbazyl have been reported, which demonstrates that carbazole plays a crucial role for the precise control of the structure and properties of EP films.[40–43] These advantageous properties arouse interests in constructing electro-active AIE molecules. Applying AIE-active derivative as a precursor to prepare the luminescent network film was recently reported by Liu et al.,[44] in which OLEDs using these films as light emitting layers exhibited a maximum luminance of 489 cd m^{-2} and a maximum luminance efficiency (LE) of 0.38 cd A^{-1}. In present work, we further develop an electro-active carbazole functionalized TPE derivative, **TPE-DFCz**, and a cross-linked electrochemically polymerized film with high quantum efficiency, smooth surface, and good thermal stability is obtained through EP method. A significantly improved performance in OLEDs using **TPE-DFCz**-based EP film as active layer is achieved with a maximum luminance of 3200 cd m^{-2} and a maximum LE of 1.16 cd A^{-1}. The result indicates that electrochemical synthesis can be a new facile route for constructing the cross-linked polymer luminescent films with AIE-activity and afford high performance in OLEDs.

EXPERIMENTAL

Instrumentation

All the reagents were purchased from Acros, J&K and Aldrich Chemical Co. and used as received. THF was dried and purified by fractional distillation over sodium in the presence of benzophenone. The supporting electrolyte, tetrabutylammonium hexafluorophosphate ($TBAPF_6$, 99%) was purchased from J&K and dried for 24 h under vacuum before use. Solvents for electrochemical experiments were the mixture of acetonitrile and CH_2Cl_2 (v/v = 1:1), which were carefully purified and purged by dry nitrogen prior to the electrochemical measurements.

The ^{1}H NMR were recorded on a Bruker AVANCE 500 spectrometers at 500 MHz at 298 K using deuterated dimethyl sulfoxide (DMSO-d_6) and $CDCl_3$ as solvents and tetramethylsiane (TMS) as internal standard. All of the compounds were characterized by a Flash EA 1112, CHNS elemental analysis instrument. The MALDI-TOF-MS mass spectra were recorded using an AXIMA-CFRTM plus instrument. UV-Vis absorption spectra were measured on Shimadzu UV-3100PC spectrophotometer, and fluorescence recorded by using a RF-5301PC. Differential scanning calorimetry (DSC) analysis was carried out using a TAQ100 instrument at 10 °C min^{-1} while flushing with nitrogen. Thermal gravimetric analysis (TGA) was recorded on a Perkin Elmer thermal analysis system at a heating rate of 10 °C min^{-1} and a nitrogen flow rate of 80 mL min^{-1}. The atomic force microscopy (AFM) images were recorded by a Seiko SPA 300 in contact mode (AFM mode). The transmission electron microscopy studies (TEM) were performed by JEM-2100F TEM instrument. The cyclic voltammetry (CV) were performed using a standard one-compartment, three-electrode electrochemical cell attached to an Electrochemical Workstation named Model CHI-660C, Shanghai, Chenhua. ITO (1.2 cm × 2.5 cm) was used as the working electrode, an Ag/Ag^+ electrode was used as the reference electrode and titanium metal was used as the counter electrode with area of 2 cm × 4 cm. **TPE-DFCz** (1 mg mL^{-1}) and $TBAPF_6$ (0.1 M) were dissolved in a mixed solvent of acetonitrile and CH_2Cl_2 (v/v = 1:1). The EP films were prepared by the CV mode, in which the thickness of the EP film can be easily controlled by scan cycles and scan rates, such as about 2.7 nm per cycle and about 27 nm as 10 cycles at a scan rate of 100 mV s^{-1}. After the EP process, the resulting EP film was washed with a mixture of acetonitrile and CH_2Cl_2 (v/v = 1:1) to remove any unreacted precursors and supporting electrolytes and then dried in a vacuum oven.

Device Fabrication

The ITO-coated glass substrates were cleaned in an ultrasonic bath with purified water, isopropylalcohol, acetone, toluene, acetone, isopropyl alcohol, respectively, and cleaned for 20 min by exposure to UV-ozone. The EP films were used as emitting layers, then TPBi, as both a hole-blocking layer and an electron-transporting layer, was thermally deposited onto the emitting layers under vacuum with a back pressure of 10^{-5} Pa. Finally, LiF buffer layer and an Al cathode were deposited onto TPBi. The luminance-current characteristics of devices were measured using a PR650 spectroscan spectrometer, and current-voltage characteristics were recorded by a Keithley 2400 sourcemeter. All of procedure was performed at room temperature under ambient conditions.

Synthesis of 1,2-*Bis*(4-bromophenyl)-1,2-Diphenylethene (2)

4-Bromobenzophenone (**1**) (11.50 g, 19.20 mmol), zinc dust (2.50 g, 38.20 mmol) and THF (100 mL) were put into a 250 mL two-necked round-bottom flask equipped with a reflux condenser. $TiCl_4$ (2.1 mL, 19.20 mmol) was dropped slowly using a syringe under nitrogen protection. The mixture was slowly warmed to room temperature and then refluxed for 12 h. Water was added to quench the reaction. The organic layer was washed and extracted with chloroform. And then compound **2** (3.60 g) was isolated by column chromatography using hexane as eluent. Yield: 76%.

^{1}H NMR (500 MHz, $CDCl_3$): δ 7.29 (d, J = 2.4 Hz, 1H), 7.28 – 7.27 (m, 1H), 7.26–7.23 (m, 3H), 7.16 (dd, J = 5.9, 2.5 Hz, 4H), 7.14–7.11 (m, 4H), 7.02 (dd, J = 5.0, 4.2, 1.9 Hz, 5H), 6.94–6.88 (m, 5H). MALDI-TOF-MS: m/z: $[M + H]^+$ calcd. for: $C_{26}H_{18}Br_2$ 490.24; found: 491.50.

Synthesis of 9,9'-((2-(4,4,5,5-tetramethyl-1,3,2-dioxaborolan-2-yl)−9H-fluorene-9,9-diyl) bis(hexane-6,1-diyl))bis(9H-carbazole) (6)

A mixture of **5** (3.72 g, 5.00 mmol), potassium acetate (3.92 g, 40 mmol), 4,4,4',4',5,5,5',5'-octamethyl-2,2'-bi(1,3,2-dioxaborolane)

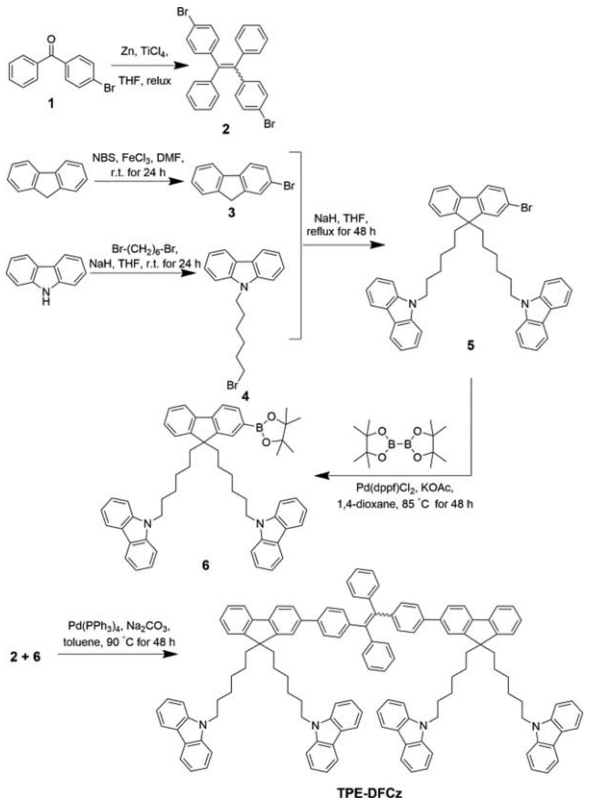

SCHEME 1 The synthetic routes to **TPE-DFCz**.

(1.90 g, 7.50 mmol), and Pd(dppf)Cl_2 (82.00 mg, 0.10 mmol) were refluxed in 1,4-dioxane (30 mL) under nitrogen. After 48 h, the mixture was cooled and the reaction was stopped. The organic layer was extracted with dichloromethane, washed with water and dried over anhydrous $MgSO_4$ overnight. After evaporating the solvent, the crude product was purified by column chromatography using petroleum ether/CH_2Cl_2 as the eluent to afford a white solid (3.16 g). Yield: 80%.

^{1}H NMR (500 MHz, $CDCl_3$): δ 8.10 (d, $J = 7.7$ Hz, 1H), 7.84 (d, $J = 7.5$ Hz, 1H), 7.73 (dd, $J = 13.0$, 6.8 Hz, 1H), 7.45 (dd, $J = 7.9$, 7.3 Hz, 1H), 7.33 (dd, $J = 13.4$, 7.6 Hz, 1H), 7.26 (t, $J = 6.0$ Hz, 1H), 7.23 (dd, $J = 13.1$, 5.7 Hz, 1H), 4.17 (t, $J = 7.3$ Hz, 1H), 3.74 (s, 1H), 2.04–1.85 (m, 1H), 1.74–1.63 (m, 1H), 1.55 (d, $J = 30.5$ Hz, 1H), 1.43 (d, $J = 33.2$ Hz, 2H), 1.33–1.22 (m, 1H), 1.21–1.01 (m, 1H). MALDI-TOF-MS: *m/z*: $[M + H]^+$ calcd. for: $C_{55}H_{59}BN_2O_2$ 790.90; found: 791.20.

Synthesis of TPE-DFCz

2 (980.48 mg, 2.00 mmol), **6** (3.16 g, 4.00 mmol), and Pd(PPh_3)$_4$ (92.40 mg, 0.08 mmol) were added to a solution of Na_2CO_3 (2.0 M) in a 3:2 (v/v) mixture of toluene/water. The mixture was stirred at 90 °C for 48 h under a nitrogen atmosphere. Subsequently, water was added to quench the reaction. The organic phase was extracted several times with chloroform, and then was dried over anhydrous $MgSO_4$ overnight. After filtration and solvent evaporation, the liquid was purified by column chromatography using petroleum ether/CH_2Cl_2 as the eluent to afford a yellow-green solid (1.82 g). Yield: 55%.

^{1}H NMR (500 MHz, $CDCl_3$): δ 8.09 (d, $J = 7.7$ Hz, 1H), 8.06 (d, $J = 7.7$ Hz, 1H), 7.71 (dd, $J = 7.6$, 4.7 Hz, 1H), 7.66 (d, $J = 6.1$ Hz, 1H), 7.64 (d, $J = 3.4$ Hz, 1H), 7.62 (s, 1H), 7.55 (d, $J = 7.9$ Hz, 1H), 7.49 (t, $J = 8.9$ Hz, 1H), 7.47–7.43 (m, 1H), 7.43–7.39 (m, 1H), 7.39–7.35 (m, 1H), 7.33–7.30 (m, 2H), 7.25 (dd, $J = 8.9$, 4.0 Hz, 2H), 7.23 (dd, $J = 7.9$, 3.3 Hz, 2H), 7.20 (s, 1H), 7.17 (dd, $J = 12.7$, 7.2 Hz, 3H), 7.15–7.07 (m, 1H), 4.17 (t, $J = 7.2$ Hz, 1H), 4.10 (t, $J = 7.2$ Hz, 1H), 1.94 (d, $J = 8.0$ Hz, 1H), 1.91 (d, $J = 5.5$ Hz, 1H), 1.88 (d, $J = 8.3$ Hz, 1H), 1.69 (dd, $J = 14.5$, 7.3 Hz, 1H), 1.63 (dd, $J = 15.5$, 8.4 Hz, 1H), 1.57 (s, 1H), 1.15 (d, $J = 6.9$ Hz, 1H), 1.10 (dd, $J = 18.3$, 11.5 Hz, 2H), 1.05 (d, $J = 7.2$ Hz, 1H), 0.64 (s, 1H),

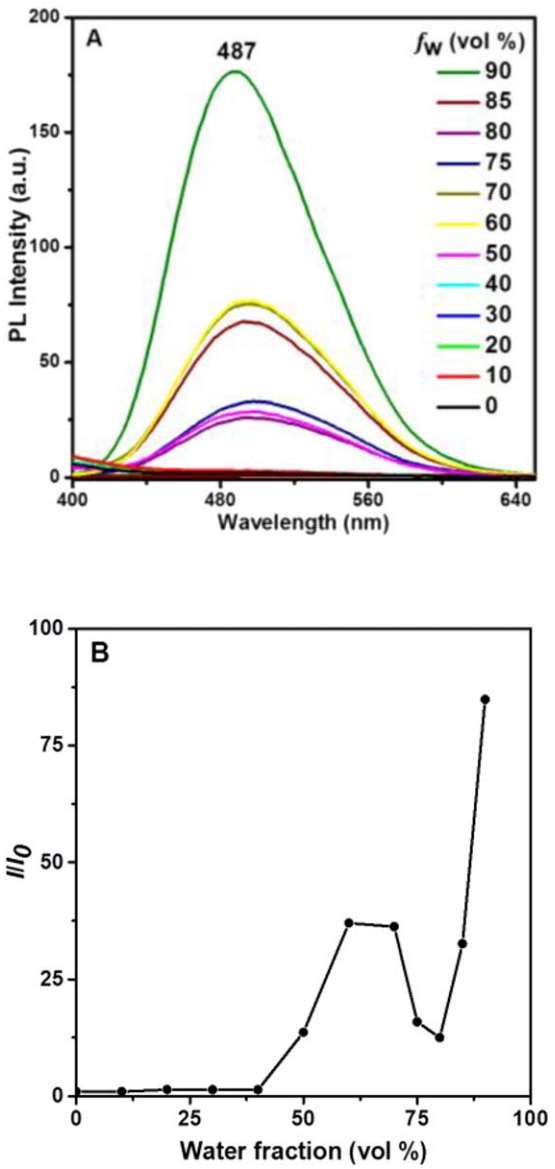

FIGURE 1 (A) PL spectra of **TPE-DFCz** in THF-water mixtures with different water fractions (f_w); (B) plot of the relative PL intensity (I/I_0) versus the compositions of THF-water mixtures of **TPE-DFCz**. I_0 and I were the maximum PL intensity of **TPE-DFCz** in pure THF and in THF-water mixtures (10 μM), respectively. Excitation wavelength: 345 nm.

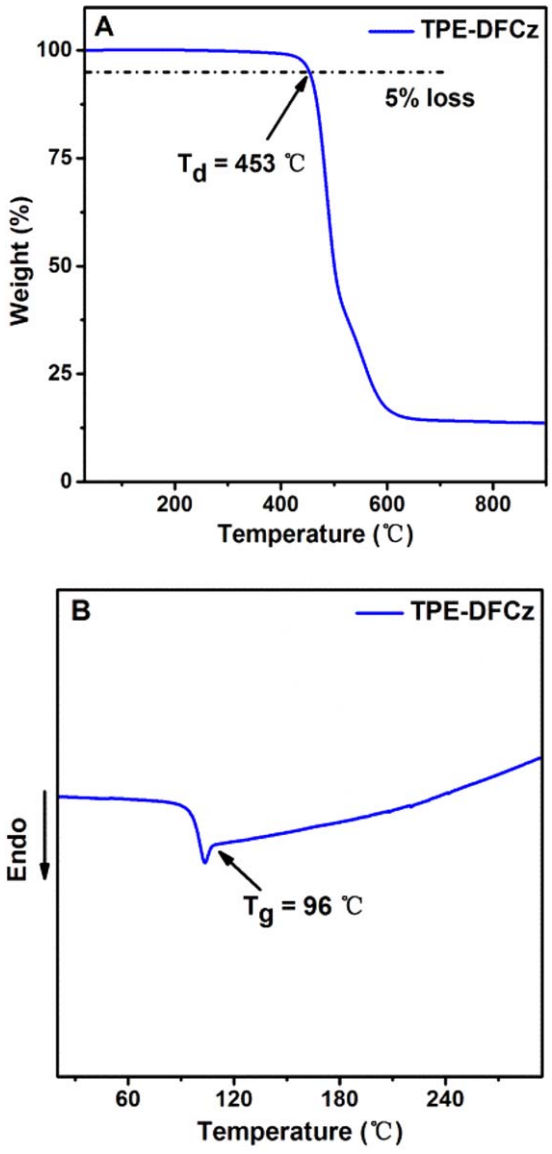

FIGURE 2 Thermal properties of **TPE-DFCz**. (A) The TGA graph of **TPE-DFCz** (heating rate: 10 °C min^{-1} under a nitrogen flow); (B) DSC graph of **TPE-DFCz** (second heating curve, heating rate: 10 °C min^{-1} under a nitrogen flow).

0.64–0.59 (m, 1H), 0.57 (d, $J = 7.3$ Hz, 1H). ^{13}C NMR (126 MHz, $CDCl_3$): δ 148.33, 144.85, 143.12, 140.27, 138.30, 131.98, 129.69, 126.22, 124.24, 123.61, 121.64, 121.32, 118.16, 110.74, 107.58, 106.48, 104.19, 101.03, 97.87, 63.13, 59.42, 56.02, 52.86, 34.46, 33.04, 28.23, 25.62, 24.20, 22.15. MALDI-TOF-MS: *m/z*: $[M + H]^+$ Calcd. for: $C_{124}H_{112}N_4$ 1658.29; found: 1659.90. ANAL. CALCD. for $C_{124}H_{112}N_4$: C, 89.81; H, 6.81; N, 3.38; found: C, 89.66; H, 6.82; N, 3.36.

RESULTS AND DISCUSSION

Scheme 1 describes the synthesis routes of **TPE-DFCz**. To begin with, dibromotetraphenylethylene (**2**) was prepared via McMurry coupling reaction using the 4-bromobenzophenone (**1**) as the starting material in the presence of zinc and $TiCl_4$. Subsequently, monomer **6** was synthesized starting from commercially available fluorene and carbazole through a three-step reaction according to our reported literatures.[45,46] With monomer **2** and **6** in hand, **TPE-DFCz** was obtained through Suzuki coupling reaction in a heterogeneous system using $Pd(PPh_3)_4$ as a catalyst. The crude product was washed with acetic acid and then purified through chromatography to give target compound as yellow-green solid with good yield of

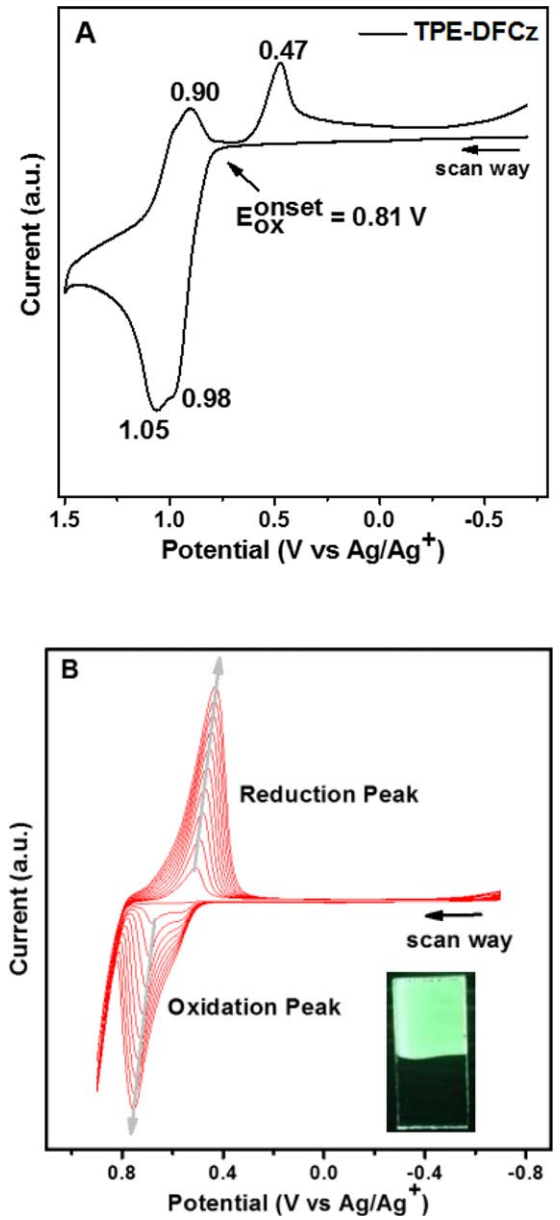

FIGURE 3 (A) CV profile of 1st cycle of **TPE-DFCz** in acetonitrile/CH_2Cl_2 (v/v = 1:1) in the presence of $TBAPF_6$ (0.1 M) electrolyte at room temperature under nitrogen protection. Scan rate: 100 mV/s; Scan range: −0.5 to 1.4 V. (B) CV profiles (1st to 10th cycles) of **TPE-DFCz** in acetonitrile/CH_2Cl_2 (v/v = 1:1) in the presence of $TBAPF_6$ (0.1 M) electrolyte at room temperature under nitrogen protection. Scan rate: 100 mV/s; Scan range: −0.7 to 0.9 V. Inset: EP film on the electrode under UV light.

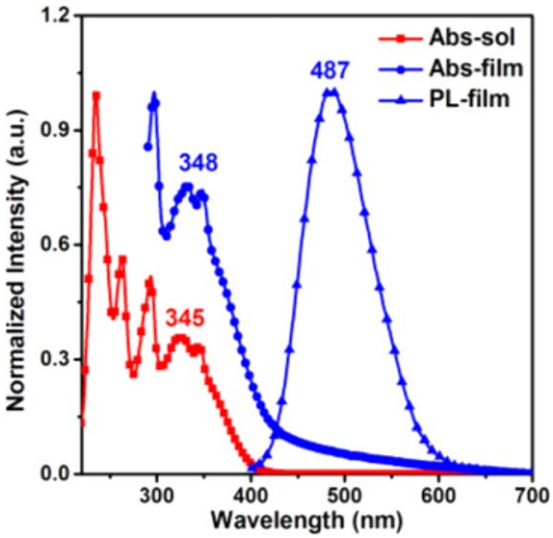

FIGURE 4 The normalized UV-Vis spectra and PL spectra of **TPE-DFCz** in dilute THF solution (concentration: 10 μM) and in thin film spin-coated from 10^{-3} M THF solution at 1500 rpm. Excitation wavelength: 350 nm.

55%. **TPE-DFCz** was characterized by MS, NMR spectra, elemental analysis, and corresponded well with its expected structure.

TPE-DFCz showed typical AIE-active spectral behavior, that is, it had no emission when dissolved in THF but exhibited intense emission in the aggregated state. Only a weak PL signal was recorded even when the water fraction (f_w) was as high as 40% because the molecules still remained dissolved in the mixture (Fig. 1). However, when f_w was higher than 50%, addition of even a small amount of water gave significant increase in the PL intensity. After reaching a maximum intensity at 60% water fraction, the PL intensity decreased with increasing water content. Then, a further increase of the water fraction was observed which resulted in a continuous increase of PL intensity. This phenomenon was often found in the characterization of the AIE effect, which might be related to the various kinds of nanoparticle suspensions.[47] Generally speaking, crystal particles lead to an enhancement in the PL intensity, while the amorphous particles result in a reduction in intensity (Supporting Information Fig. S1).[48] The observed overall PL intensity data would depend on the combined results of the two kinds of nanoparticles, which manifested no regularity in high water contents of **TPE-DFCz**. From the THF solution to the aggregated suspension in the 90% aqueous mixture, the maximum PL peak intensity was increased up to 84 times due to the restriction of molecular motions confirming its AIE-active nature. This process was also reflected by the corresponding PL spectrum at low temperature of 77 K, in which the emission intensity was 437-folded higher than the emission recorded at room temperature (Supporting Information Fig. S2).

The thermal properties of **TPE-DFCz** were investigated using thermogravimetric analysis (TGA) and differential scanning calorimetry (DSC) under a nitrogen atmosphere. DSC result indicated that **TPE-DFCz** exhibited glass transition temperature (T_g) at 96 °C in the experimental temperature range (Fig. 2).

This is a relatively high value among the solution-processable small molecule containing flexible dihexyl side chains. Specially, no crystallization or phase transition was observed. The decomposition temperature (T_d) was measured to be at 453 °C due to its high molecular weight. The TGA and DSC characterization demonstrated **TPE-DFCz** possessed high thermal stability which is desirable for its application in solid state.

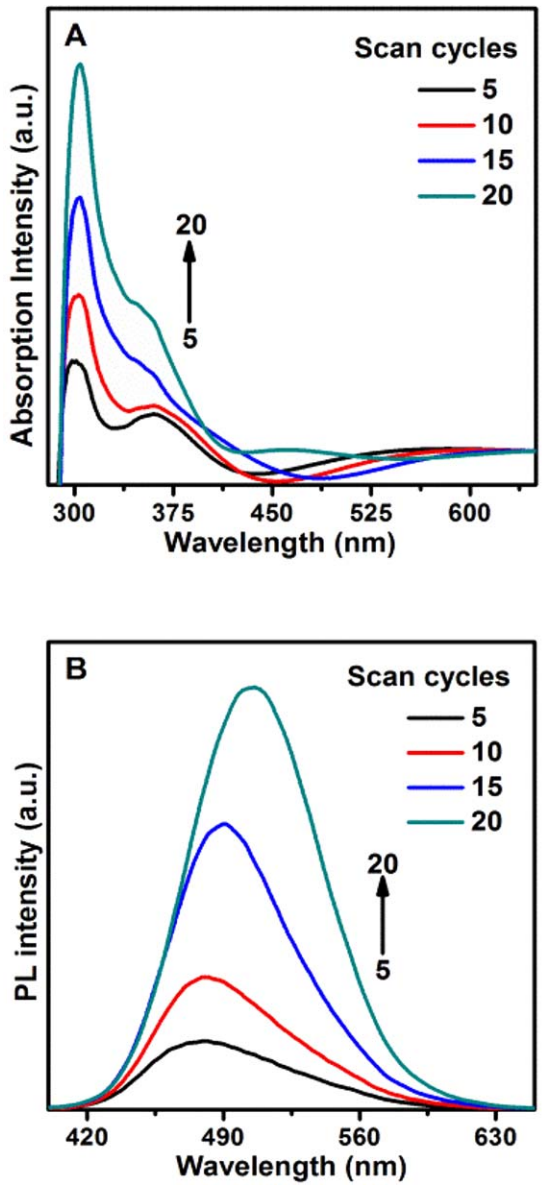

FIGURE 5 The absorption (A) and PL (B) spectra of EP films on ITO using different scan cycles. The EP films are prepared using $TBAPF_6$ (0.1 M) as the supporting electrolyte at a scan rate of 100 mV/s and a scan range of −0.7 to 0.9 V.

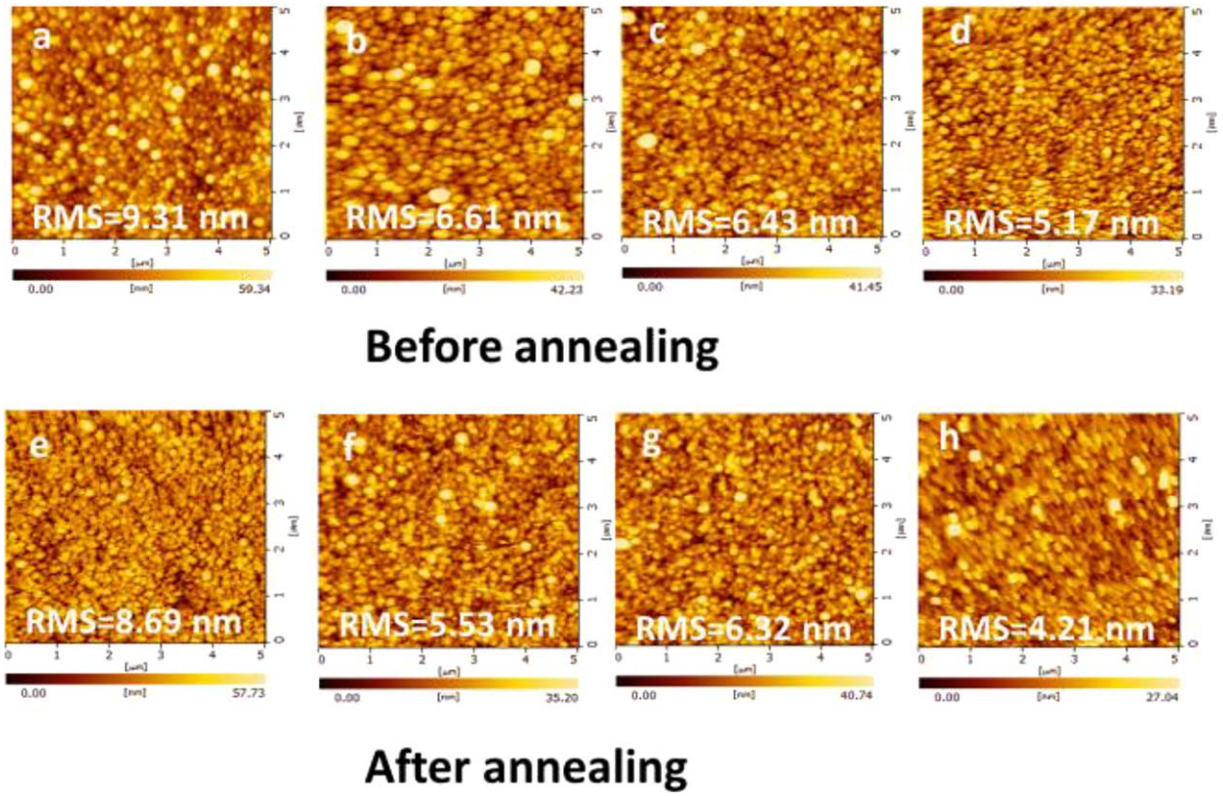

FIGURE 6 AFM images showing 5 μm $\times$ 5 μm areas of EP films of **TPE-DFCz** on ITO. The EP films were prepared at the scan rate of 100 mV/s using $TBAPF_6$ with different scan cycles. (a–d were 5, 10, 15, and 20 scan cycles, respectively, under room temperature; e–h after heating at 120 °C for 20 min.).

Cyclic voltammetry (CV) was employed to investigate the electrochemical behaviour of **TPE-DFCz**. Film of **TPE-DFCz** was fabricated by multicycled cyclic voltammetry (CV) in a mixture of acetonitrile and CH_2Cl_2 (v/v = 1:1) containing the electrolyte with **TPE-DFCz** concentration of 6.03×10^{-4} mol L^{-1}. From the first cycle of a positive CV scan in the potential sweep between -0.5 and 1.4 V [Fig. 3(A)], the onset oxidative potential of **TPE-DFCz** appeared at 0.81 V, which was attributed to the oxidation of carbazole. As the scan potential higher than 0.81 V, the anodic current increased rapidly and yielded a potential peak at 0.98 V, which indicated that more carbazole groups were oxidized. Previous studies have shown that the carbazole transformed into cationic radicals during oxidation and then couples effectively with each other to form dimeric carbazole cations.[12,49] During the negative scan, an obvious reductive peak was observed at the potential of 0.47 V, assigning to the reduction of the dimeric carbazole cation. In contrast, the oxidation and reduction peaks of the TPE core were observed at potentials of 1.05 and 0.98 V, respectively. This clear difference in oxidation potentials between TPE unit and carbazole groups was of vital importance because it guaranteed that polymerization could occur only at the peripheral carbazole groups, whereas the TPE unit remained untouched.

From the second scan in the continuous CV curves as shown in Figure 3(B), a new peak appeared at 0.68 V, which was owing to the oxidation of the formed dimeric carbazoles. Recurrent sweeps resulted in a progressive increase of the peak current, indicating the occurrence of the coupling reaction between the carbazole units and the growth of the EP film on the electrode. After 10 cycles, a transparent film was formed on the electrode which exhibited green emitting color under UV light. The resulting cross-linked film was highly robust and insoluble in any organic solvents.

Figure 4 shows the absorption spectra of **TPE-DFCz** in dilute THF solution and in thin films formed on quartz substrates by spin-coating method. The absorption spectrum of **TPE-DFCz** in THF solution was characterized by several absorption peaks at 345, 327, 292, 264, and 231 nm, which was the combination of TPE, carbazole and dihexylfluorene groups. The 345 nm low-energy band was attributed to the π-π^* electronic transitions in the backbone, which was similar as that observed for other fluorene-based oligomers.[46,50] The absorption peak at 327 nm could be assigned to the π-π^* transitions of TPE. The high-energy band emerged at 292, 264, and 231 nm was from the peripheral carbazole groups.[51] Similar results were also observed in the absorption spectrum of the film. The film of **TPE-DFCz** exhibited strong blue emission peaking at 487 nm with high quantum efficiency of nearly 93%.

The UV-Vis spectra of **TPE-DFCz** EP films with increased scan cycles were presented in Figure 5(A). EP films were

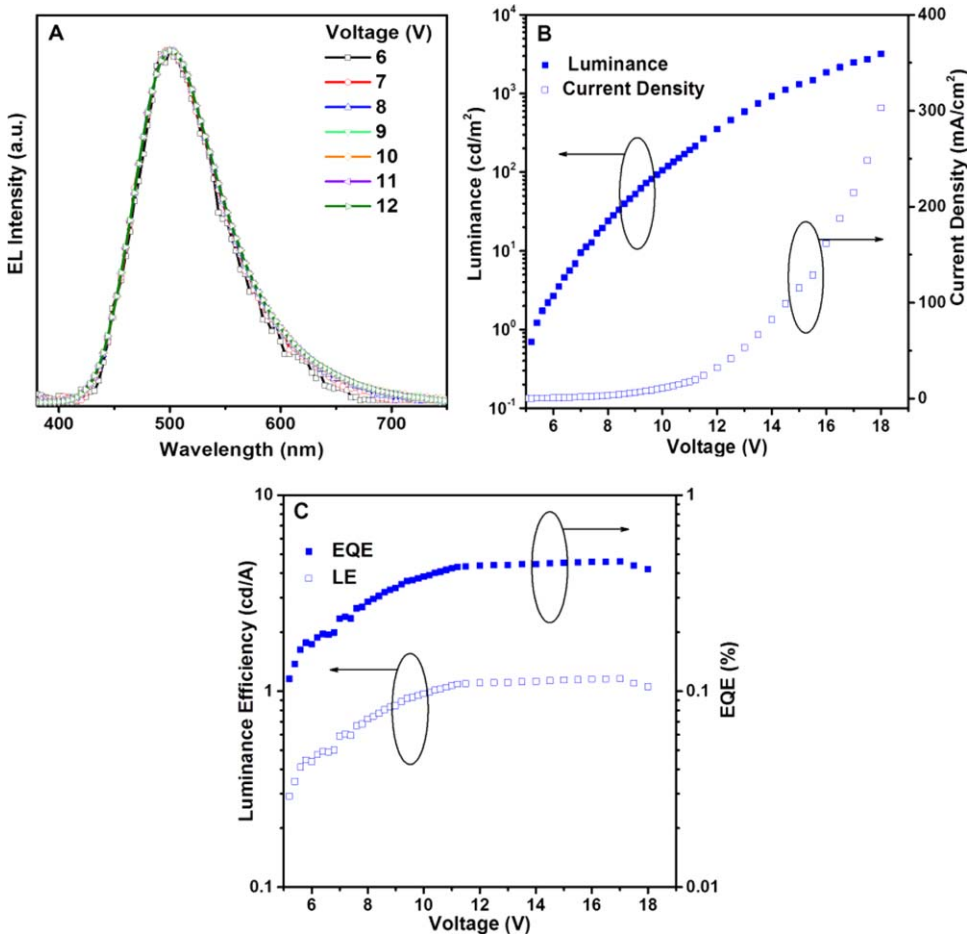

FIGURE 7 (A) EL spectra of the solid thin film of **TPE-DFCz** recorded in the voltage from 6 to 12 V. (B) Luminance efficiency-voltage-current density characteristics of multilayer EL devices of **TPE-DFCz**. (C) Luminance efficiency-Voltage-EQE characteristics of multilayer EL devices of **TPE-DFCz**.

prepared at the scan rate of 100 mV/s using $TBAPF_6$ with various scan cycles at the voltage from −0.7 to 0.9 V. For the spin-coated film, three absorption peaks locating at 296, 333, and 348 nm were observed. Notably, the absorption profiles of EP films became broad and red-shifted due to the π-π^* transition of dimeric carbazolyl.[37] In the EP films, a broad tail band extending from 450 to 800 nm with relatively low intensities were also appeared. This low-energy band had been already observed in other carbazole-based EP films and been thought to be relative to the dications of dimeric carbazolyl.[12,37,52] With the increased number of scan cycles, the absorption intensity was also enhanced, demonstrating that the thickness of EP films could be controlled by scan cycles.

The PL spectra of **TPE-DFCz** EP films with increased scan cycles were presented in Figure 5(B). When excited by a 350 nm light, the maximum emission wavelengths ($\lambda_{em,\ max}$) of **TPE-DFCz** EP film appeared at 477, 480, 490, and 505 nm, respectively. Comparing with **TPE-DFCz** spin-coated film, the emission maximum of the EP films were continuously red-shifted, which implied that cross-linking by EP would cause a significant increase in the conjugation extent of the molecules originating from the closer molecular packing. Similarly, the PL intensity was also enhanced with the increased number of scan cycles. The EP film showed high quantum efficiencies due to the AIE nature. The quantum efficiencies scanned by 5 to 20 cycles were measured to be 63%, 40%, 32%, 30%, respectively. It can be seen that the efficiency was gradually reduced with the continuously increased scan cycles. This might be due to the left residual charged ion species within the films during electrochemical deposition process and would decrease the quantum efficiency. This effect became more severe in the resultant thicker films when scanned with more cycles.

The morphologies of EP films prepared with different scan cycles under room temperature and after thermal annealing 120 °C for 20 min were studied by AFM, respectively. The root mean square roughness (RMS) of the EP films prepared in the optimal potential became gradually smaller with the increased scan cycles as shown in Figure 6. For example, the RMS is 9.31 nm when scanned for five cycles and 5.176 nm for 20 cycles under room temperature. The values for these EP films were relatively higher than other system as reported by Liu et al.[44] It might have the same origin that

electrochemical deposition would leave residual charged ion species within the film and resulted in rougher surface. After thermal annealing, the films became more uniform with decreased RMS values, which was comparable to the results reported before. Thermal annealing process is an efficient and simple method for suppressing the negligible effect of counter ions in the EP films, which was also applied for the OLED fabrication in this work.

The high luminescence of the cross-linked **TPE-DFCz** ED films ensured the fabrication of ED-film-based PLEDs. The optimized double-layer device was prepared with the following structure of ITO/ED film (27 nm)/TPBi (40 nm)/LiF (0.5 nm)/Al (100 nm), in which ITO-coated glass was used as both the substrate and anode, TPBi as both a hole-blocking layer and an electron-transporting layer, and LiF as the modificatory layer of the cathode Al. All the characterization data for devices were summarized in Supporting Information Table S1. The EP film scanned by 10 cycles was applied as the active layer due to the appropriate thickness, optimized quantum efficiency and surface roughness. Figure 7(B) presents the EL spectra and the luminous-efficiency—voltage–current-density characteristics of the device. **TPE-DFCz** EP device showed green emission with an emissive peak at 500 nm in the EL spectra and CIE coordinates of (0.237, 0.430). The EL spectrum of device was consistent with its PL spectrum of EP film. The emission spectra were kept unchanged when the voltages varied from 6 to 12 V indicating the good stability of cross-linked film as active layer. The EP device exhibited a turn-on voltage of 5.4 V, a maximum brightness of 3200 cd m^{-2}, an external quantum efficiency of 0.46% and a LE of 1.16 cd A^{-1}, which was a relatively high level in the double-layer PLEDs. The efficiencies showed very low roll-off indicating the excellent stability of the EP film. The performance of the device in the present work was significantly improved as compared to previously reported data.[44] The result indicated that cross-linked polymer network films of based on TPE can be used as good emitters in the construction of EL devices. We also believe further optimization of the **TPE-DFCz** EP film by reducing the residue of cations can lead to a better device performance. Besides such polymer EP films can also have potential applications in solar cells to be acted as the active layers or interfacial layers.

CONCLUSIONS

In conclusion, a new AIEgen, **TPE-DFCz**, containing TPE core and a peripheral carbazole functional groups is synthesized and well characterized. A cross-linked electrochemically polymerized film is successfully created and CV behavior, fluorescent spectra, thermal properties, AFM characterization of the EP film are performed. The resultant EP film exhibits high quantum efficiency of 63%, good thermal stability, smooth surface morphology after annealing. The effect of various scan cycles on the luminescent property is investigated which demonstrated that **TPE-DFCz** films show red-shifted emission spectra and reduced quantum efficiencies with the increased scan cycles. The results illustrate that the efficiencies and surface smoothness of the films can be conveniently tuned by the scan cycles. The double-layer OLED using EP film as active layer achieves a maximum luminance of 3200 cd m^{-2}, a LE of 1.16 cd A^{-1} and an external quantum efficiency of 0.46%. The electrochemical synthesis could be a novel way to fabricate the cross-linked polymer films with AIE molecules.

ACKNOWLEDGMENTS

This research is supported by the Ministry of Science and Technology of China (2013CB834801, 2016YFB0401001), the National Science Foundation of China (21374038), and the Jilin Provincial Science and Technology Department (20160101302JC).

REFERENCES AND NOTES

1 R. H. Friend, R. W. Gymer, A. B. Holmes, J. H. Burroughes, R. N. Marks, C. Taliani, D. D. C. Bradley, D. A. D. Santos, J. L. Bredas, M. Logdlund, W. R. Salaneck, *Nature* **1999**, *397*, 121–128.

2 H. Uoyama, K. Goushi, K. Shizu, H. Nomura, C. Adachi, *Nature* **2012**, *492*, 234–238.

3 W. Z. Yuan, Y. Y. Gong, S. M. Chen, X. Y. Shen, J. W. Y. Lam, P. Lu, Y. W. Lu, Z. M. Wang, R. R. Hu, N. Xie, H. S. Kwok, Y. M. Zhang, J. Z. Sun, B. Z. Tang, *Chem. Mater.* **2012**, *24*, 1518–1528.

4 G. Z. Xie, X. L. Li, D. J. Chen, Z. H. Wang, X. Y. Cai, D. C. Chen, Y. C. Li, K. K. Liu, Y. Cao, S. J. Su, *Adv. Mater.* **2016**, *28*, 181–187.

5 J. S. Kim, B. J. Kim, Y. J. Choi, M. H. Lee, M. S. Kang, J. H. Cho, *Adv. Mater.* **2016**, *28*, 4803–4810.

6 S. Watanabe, T. Fujita, J. C. Ribierre, K. Takaishi, T. Muto, C. Adachi, M. Uchiyama, T. Aoyama, M. Matsumoto, *ACS Appl. Mater. Interfaces* **2016**, *8*, 17574–17582.

7 I. Cho, S. K. Park, B. Kang, J. W. Chung, J. H. Kim, K. Cho, S. Y. Park, *Adv. Funct. Mater.* **2016**, *26*, 2966–2973.

8 J. Deng, Y. X. Xu, L. Q. Liu, C. F. Feng, J. Tang, Y. Gao, Y. Wang, B. Yang, P. Lu, W. S. Yang, Y. G. Ma, *Chem. Commun.* **2016**, *52*, 2370–2373.

9 H. D. de Gier, F. Jahani, R. Broer, J. C. Hummelen, R. W. Havenith, *J. Phys. Chem. A* **2016**, *120*, 4664–4671.

10 S. Q. Zhang, L. Ye, J. H. Hou, *Adv. Energy Mater.* **2016**, *6*, 1502529.

11 S. Jinnai, Y. Ie, M. Karakawa, T. Aernouts, Y. Nakajima, S. Mori, Y. Aso, *Chem. Mater.* **2016**, *28*, 1705–1713.

12 M. Li, S. Tang, F. Shen, M. Liu, W. J. Xie, H. Xia, L. L. Liu, L. L. Tian, Z. Q. Xie, P. Lu, M. Hanif, D. Lu, G. Cheng, Y. G. Ma, *J. Phys. Chem. B* **2006**, *110*, 17784–17789.

13 M. Li, S. Tang, D. Lu, F. Z. Shen, M. R. Liu, H. Wang, P. Lu, M. Hanif, Y. G. Ma, *Semiconductor Sci. Technol.* **2007**, *22*, 855–858.

14 Z. K. Fan, N. Q. Li, Y. W. Quan, Q. M. Chen, S. H. Ye, Q. L. Fan, W. Huang, *J. Polym. Sci. Part A: Polym. Chem.* **2016**, *54*, 795–801.

15 B. J. de Gans, P. C. Duineveld, U. S. Schubert, *Adv. Mater.* **2004**, *16*, 203–213.

16 S. Tang, M. R. Liu, C. Gu, Y. Zhao, P. Lu, D. Lu, L. L. Liu, F. Z. Shen, B. Yang, Y. G. Ma, *J. Org. Chem.* **2008**, *73*, 4212–4218.

17 C. Gu, T. Fei, Y. Lv, T. Feng, S. F. Xue, D. Lu, Y. G. Ma, *Adv. Mater.* **2010**, *22*, 2702–2705.

18 H. H. Zhang, Y. N. Zhang, C. Gu, Y. G. Ma, *Adv. Energy Mater.* **2015**, *5*, 1402175.

19 H. R. Nie, Y. Lv, L. Yao, Y. Y. Pan, Y. Zhao, P. Li, G. N. Sun, Y. G. Ma, M. Zhang, *J. Hazard. Mater.* **2014**, *264*, 474–480.

20 C. Gu, W. Y. Dong, L. Yao, Y. Lv, Z. B. Zhang, D. Lu, Y. G. Ma, *Adv. Mater.* **2012**, *24*, 2413–2417.

21 C. Gu, Y. C. Chen, Z. B. Zhang, S. F. Xue, S. H. Sun, K. Zhang, C. M. Zhong, H. H. Zhang, Y. Y. Pan, Y. Lv, Y. Q. Yang, F. H. Li, S. B. Zhang, F. Huang, Y. G. Ma, *Adv. Mater.* **2013**, *25*, 3443–3448.

22 C. Gu, Y. C. Chen, Z. B. Zhang, S. F. Xue, S. H. Sun, C. M. Zhong, H. H. Zhang, Y. Lv, F. H. Li, F. Huang, Y. G. Ma, *Adv. Energy Mater.* **2014**, *4*, 1301771.

23 C. Gu, Z. B. Zhang, S. H. Sun, Y. Y. Pan, C. M. Zhong, Y. Lv, M. Li, K. Ariga, F. Huang, Y. G. Ma, *Adv. Mater.* **2012**, *24*, 5727–5731.

24 M. Li, J. Zhang, H. J. Nie, M. Liao, L. Sang, W. Qiao, Z. Y. Wang, Y. G. Ma, Y. W. Zhong, K. Ariga, *Chem. Commun.* **2013**, *49*, 6879–6881.

25 Y. Lv, L. Yao, C. Gu, Y. X. Xu, D. D. Liu, D. Lu, Y. G. Ma, *Adv. Funct. Mater.* **2011**, *21*, 2896–2900.

26 C. Gu, N. Huang, Y. Wu, H. Xu, D. L. Jiang, *Angew. Chem. Int. Ed. Engl.* **2015**, *54*, 11540–11544.

27 C. Favre, L. Abello, D. Delabouglise, *Adv. Mater.* **1997**, *9*, 722–725.

28 C. Gu, N. Huang, Y. C. Chen, L. Q. Qin, H. Xu, S. T. Zhang, F. H. Li, Y. G. Ma, D. L. Jiang, *Angew. Chem. Int. Ed. Engl.* **2015**, *54*, 13594–13598.

29 Y. N. Hong, J. W. Y. Lam, B. Z. Tang, *Chem. Soc. Rev.* **2011**, *40*, 5361–5388.

30 J. D. Luo, Z. L. Xie, J. W. Y. Lam, L. Cheng, H. Y. Chen, C. F. Qiu, H. S. Kwok, X. W. Zhan, Y. Q. Liu, D. B. Zhu, B. Z. Tang, *Chem. Commun.* **2001**, 1740–1741.

31 Y. Q. Dong, J. W. Y. Lam, A. J. Qin, J. Z. Liu, B. Z. Tang, J. X. Sun, H. S. Kwok. *Appl. Phys. Lett.* **2007**, *91*, 011111–011113.

32 Y. L. Liu, T. Shan, L. Yao, Q. Bai, Y. Guo, J. Y. Li, X. Han, W. J. Li, Z. M. Wang, B. Yang, P. Lu, Y. G. Ma, *Org. Lett.* **2015**, *17*, 6138–6141.

33 J. Mei, N. L. Leung, R. T. Kwok, J. W. Y. Lam, B. Z. Tang, *Chem. Rev.* **2015**, *115*, 11718–11940.

34 Z. J. Zhao, C. M. Deng, S. M. Chen, J. W. Y. Lam, W. Qin, P. Lu, Z. M. Wang, H. S. Kwok, Y. G. Ma, H. Y. Qiu, B. Z. Tang, *Chem. Commun.* **2011**, *47*, 8847–8849.

35 M. I. Mangione, R. A. Spanevello, D. Minudri, D. Heredia, L. Fernandez, L. Otero, F. Fungo, *Electrochim. Acta.* **2016**, *207*, 143–151.

36 H. Liu, Q. Bai, L. Yao, D. H. Hu, X. Y. Tang, F. Z. Shen, H. H. Zhang, Y. Gao, P. Lu, B. Yang, Y. G. Ma, *Adv. Funct. Mater.* **2014**, *24*, 5881–5888.

37 Z. H. Wei, J. K. Xu, G. M. Nie, Y. K. Du, S. Z. Pu, *J. Electroanal. Chem.* **2006**, *589*, 112–119.

38 P. Marrec, C. Dano, N. Gueguen-Simonet, J. Simonet, *Synth. Met.* **1997**, *89*, 171–179.

39 Y. Y. Shen, H. M. Miao, J. K. Xu, H. L. Zhang, B. Y. Lu, *Acta Polym. Sin.* **2008**, *1*, 1089–1095.

40 M. Li, S. Tang, F. Z. Shen, M. R. Liu, W. J. Xie, H. Xia, L. L. Liu, L. L. Tian, Z. Q. Xie, P. Lu, M. Hanif, D. Lu, C. Gu, Y. G. Ma, *Chem. Commun.* **2006**, 3393–3395.

41 H. J. Son, W. S. Han, S. J. Han, C. Lee, S. O. Kang, *J. Phys. Chem. C* **2010**, *114*, 1064–1072.

42 H. J. Son, W. S. Han, K. H. Lee, H. J. Jung, C. Lee, J. Ko, S. O. Kang, *Chem. Mater.* **2006**, *18*, 5811–5813.

43 Y. Y. Zhu, C. Gu, S. Tang, T. Fei, X. Gu, H. Wang, Z. M. Wang, F. F. Wang, D. Lu, Y. G. Ma, *J. Mater. Chem.* **2009**, *19*, 3941.

44 C. Liu, H. Y. Luo, G. Shi, J. J. Yang, Z. G. Chi, Y. G. Ma. *J. Mater. Chem. C* **2015**, *3*, 3752–3759.

45 P. Lu, J. W. Y. Lam, J. Liu, C. K. W. Jim, W. Yuan, C. Y. K. Chan, N. Xie, Q. Hu, K. K. L. Cheuk, B. Z. Tang, *Macromolecules* **2011**, *44*, 5977–5986.

46 S. Tang, M. R. Liu, P. Lu, H. Xia, M. Li, Z. Q. Xie, F. Z. Shen, C. Gu, H. Wang, B. Yang, Y. G. Ma, *Adv. Funct. Mater.* **2007**, *17*, 2869–2877.

47 X. Q. Zhang, Z. Y. Ma, Y. Yang, X. Y. Zhang, Z. G. Chi, S. W. Liu, J. R. Xu, X. R. Jia, Y. Wei, *Tetrahedron* **2014**, *70*, 924–929.

48 Z. X. Wang, H. X. Shao, J. C. Ye, L. Tang, P. Lu, *J. Phys. Chem. B* **2005**, *109*, 19627–19633.

49 C. Gu, S. Tang, B. Yang, S. J. Liu, Y. Lv, H. Wang, S. M. Yang, M. Hanif, D. Lu, F. Z. Shen, Y. G. Ma, *Electrochim. Acta* **2009**, *54*, 7006–7011.

50 Y. Geng, A. Trajkovska, D. Katsis, J. J. Ou, S. W. Culligan, S. H. Chen, *J. Am. Chem. Soc.* **2002**, *124*, 8337–8347.

51 A. Tanimoto, T. Yamamoto, *Macromolecules* **2006**, *39*, 3546–3552.

52 F. Tran-Van, T. Henri, C. Chevrot, *Electrochim. Acta* **2002**, *47*, 2927–2936.